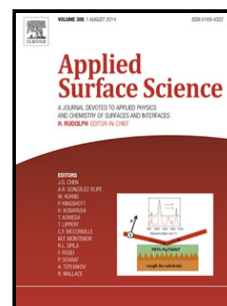# Accepted Manuscript

Title: Electrooxidation of *p*-nitrophenol using a composite organo-smectite clay glassy carbon electrode

Author: Marija J. Žunić Aleksandra D. Milutinović-Nikolić Dalibor M. Stanković Dragan D. Manojlović Nataša P. Jović-Jovičić Predrag T. Banković Zorica D. Mojović Dušan M. Jovanović

Please cite this article as: M.J. Žunić, A.D. Milutinović-Nikolić, D.M. Stanković, D.D. Manojlović, N.P. Jović-Jovičić, P.T. Banković, Z.D. Mojović, D.M. Jovanović, Electrooxidation of *p*-nitrophenol using a composite organo-smectite clay glassy carbon electrode, *Applied Surface Science* (2014), http://dx.doi.org/10.1016/j.apsusc.2014.05.228

This is a PDF file of an unedited manuscript that has been accepted for publication. As a service to our customers we are providing this early version of the manuscript. The manuscript will undergo copyediting, typesetting, and review of the resulting proof before it is published in its final form. Please note that during the production process errors may be discovered which could affect the content, and all legal disclaimers that apply to the journal pertain.

Electrooxidation of *p*-nitrophenol using a composite organo-smectite clay glassy carbon electrode

Marija J. Žunić[a*], Aleksandra D. Milutinović-Nikolić[a], Dalibor M. Stanković[b], Dragan D. Manojlović[b], Nataša P. Jović-Jovičić[a], Predrag T. Banković[a], Zorica D. Mojović[a], Dušan M. Jovanović[a]

[a]University of Belgrade- Institute of Chemistry, Technology and Metallurgy, Center for Catalysis and Chemical Engineering, Njegoševa 12, 11000 Belgrade, Republic of Serbia
[b]University of Belgrade, Faculty of Chemistry, Studentski trg 12-16, Belgrade, Republic of Serbia

ABSTRACT
Bentonite clay rich in smectite clay mineral from seldom investigated locality Mečji Do (MD) in Serbia was modified. The organomodification was performed with different loadings of benzyltrimethylammonium (BTMA) cation. The characterization of clay-based samples was performed, including XRD, FTIR and chemical and textural analysis. Electrochemical investigation was performed on a glassy carbon electrode (GCE) support with thin film of homogenously deposited either Na-enriched or one of organomodified clays forming composite electrodes. The behavior of the composite electrodes in the electrooxidation of *p*-nitrophenol (*p*-NP) in acidic media was analyzed using multisweep cyclic voltammetry. Oxidation of *p*-NP occurred at 1.2 V vs. Ag/AgCl for all investigated electrodes. The results indicate that the incorporation of BTMA cations into smectite enhanced the electrode stability toward the electrooxidation of *p*-NP in comparison to bare GCE and composite electrode based on Na-enriched clay. The current density for the *p*-NP oxidation wave slightly decreased with the increase of BTMA loading. On the other hand the electrode stability was significantly improved with the increase of BTMA loading.

* Corresponding author: Phone: +381 11 2630 213; Fax: +381-11-2637-977;
E-mail: marija.zunic@nanosys.ihtm.bg.ac.rs

Keywords: Composite electrode; Electrooxidation; *p*-nitrophenol; Benzil trimethylammonium cation; Electrode stability

1. INTRODUCTION

Phenol and its derivatives, have toxic effects on humans, animals and plants, even at very low concentrations. In particular, *p*-Nitrophenol (*p*-NP) is included in the US Environmental Protection Agency List of Priority Pollutants [1], due to its high environmental impact, toxicity and persistence. Considering that *p*-NP is widely used as intermediate in the production of herbicides, pesticides, explosives, dyes and plasticizers it is inevitably released into environment. Based on the above description, wastewater treatment and detection of *p*-NP in effluents are two major research directions [2]. Various techniques have been used for the detection of *p*-NP. Among them, spectrophotometry [3] gas chromatography [4] and high performance liquid chromatography techniques [5] are commonly used. Electrochemical methods have lately received considerable attention in the determination of nitrophenols. These methods have several advantages such as fast response, cheap instrumentation, low cost, simple operation, high sensitivity and selectivity and the possibility of in situ detection. Electrochemical determination of *p*-NP may be accomplished by oxidation on solid electrodes. The use of bare electrode has revealed the drawback of electrode fouling due to polymer formation during oxidation [2]. This problem might be avoided using chemically modified electrodes.

Chemically modified composite electrodes are a field of growing interest in electrochemistry, analytical chemistry and environmental protection. The majority of these electrodes can be obtained by chemisorption, covalent bonding and film deposition [6]. Among a wide range of electrode modifiers, inorganic materials, such as zeolites, silica-based hybrid materials and clays, have attracted the attention of electrochemists [7]. Recent papers report the investigation of clays and clay minerals as electrode materials for the detection of numerous target analytes such as 2-nitrophenol [8], methylparathion pesticide [9], mesotrione herbicide [10], etc. The two main features that evoke interest in clays are their common availability and their unique properties [11]. Clay minerals are naturally occurring, abundant, inexpensive, and environment-friendly nanomaterials. Despite these attractive properties, raw clay minerals can exhibit poor selectivity and restricted adsorption capacities [12].

2

Bentonite clay is dominantly consisted of smectite minerals. Smectite minerals are a class of ionic lamellar solids, which consist of negatively charged 2:1 aluminosilicate layers with intercalated exchangeable cations and water molecules. One of the most important properties of smectites is the cation exchange ability. Cations in the interlamellar region can be replaced with other inorganic /organic cations or organic molecules. The intercalation of quaternary alkylammonium cations in the interlamellar region of smectites results in materials with hybrid organic–inorganic interfaces (organoclays) with different surface properties in comparison with raw clay [13-15]. As a result, organoclays are powerful adsorbents for nonionic organic compounds (NOC) comparing with natural bentonite and other clays [16-18]. The adsorption properties of organoclays depend greatly on the characteristics of the exchanged organic cations [19, 20].

It is well known that organoclays are excellent adsorbents for the removal of phenolic compounds [21-23]. Shen et al. [21] demonstrated that relatively high affinity of phenol to benzyltrimethylammonium (BTMA) - bentonite is probably the consequence of favorable interaction between phenol molecules and benzene ring in BTMA ions through π-π type interactions.

One of the types of composite electrodes containing materials like clays or organoclays, are obtained by coating electrode surfaces with thin films [10, 12]. Electrode materials based on organoclays have been used for the electrochemical determination of phenolic compounds [24-26]. Since p-nitrophenol (p-NP) is an aromatic compound, the main assumption was that a BTMA-bentonite based electrode can be employed in the electrooxidation of p-NP. Bentonite clay from seldom investigated locality Mečji Do in Serbia was modified with different loadings of BTMA cation. The obtained materials were denoted as BTMA-MDs and used as electrode materials in composite electrodes. Electrochemical investigation was performed on a glassy carbon electrode (GCE) support coated with thin film of homogenously deposited clay (Na-enriched or one of BTMA-MDs). The electrodes were tested toward the electro-oxidation of p-NP. The effect of BTMA/clay ratio on the electrochemical behavior of the modified composite electrodes was investigated using Multisweep Cyclic Voltammetry (MCV).

2. EXPERIMENTAL

2.1. *Materials*

3

Bentonite clay was obtained from Mečji Do, Serbia. It was crushed, ground and sieved through a 74 μm sieve. The ignition loss was 16.1 mass %. The chemical composition (mass %) of the raw dry clay (< 74 μm) is presented in the Table 1.

Table 1. Chemical composition of raw clay from Mečji Do locality.

Sample	SiO_2	Al_2O_3	Fe_2O_3	MgO	CaO	Na_2O	K_2O	TiO_2
				mass %				
Raw clay	55.3	20.7	2.0	2.6	2.1	0.4	0.6	0.2

The following chemicals were used as received: benzyltrimethylammonium (BTMA) bromide with purity of 98% (Alfa-Aesar), *p*-NP p.a. (CIBA), Nafion® solution (5 mass % in lower aliphatic alcohols and water, with water content of 15-20 %, Sigma-Aldrich) and carbon black Vulcan XC72 (Cabot Corporation).

2.2. Preparation of composite electrode

Na-enriched bentonite (Na-MD), homoionic clay, was prepared in order to provide uniformly modified organo-bentonite. Na-MD was prepared by stirring a suspension of raw clay powder (< 74 μm) in 1 M NaCl for 24 h. This procedure was repeated three times until exchangeable cations were quantitatively replaced with Na^+. After stirring, the dispersion was washed by dialysis against deionized water until the surrounding water was Cl^- free (tested with 0.1 M $AgNO_3$). The cation exchange capacity (CEC) of Na-MD was determined by the standard ammonium acetate method [27]. The CEC was 0.795 mmol per 1 g of bentonite dried at 110 °C.

Previously described procedure [28] was used for the preparation of organoclay. The samples were prepared by drop-wise addition of appropriate amounts of BTMA bromide (0.159, 0.398, 0.795, and 1.590 mmol/g) dissolved in 150.0 cm^3 of distilled water in 100.0 cm^3 of 3 % (w/w) Na-MD suspension. After stirring during 24 h at room temperature, the dispersion was filtered through a Buchner funnel and Filtrak 388 filter paper. The obtained filter cake was washed with distilled water until the bromide test with 0.1 M $AgNO_3$ was negative. The samples were dried at 80 °C, ground and sieved through a 74 μm sieve. The amount of BTMA cations used for the preparation of

organoclay was expressed in multiples of CEC with values 0.2, 0.5, 1.0, and 2.0; hence the samples were denoted as 0.2 BTMA-MD, 0.5 BTMA-MD, 1.0 BTMA-MD, and 2.0 BTMA-MD.

Modified composite working electrode in the form of thin film on GCE was prepared by drop coating. The mixture of each clay sample and 10 mass % of carbon black was homogeneously dispersed in the original Nafion® solution using an ultrasonic bath. Film deposition was performed by dropping 5 µL of the clay dispersion onto the glassy carbon rotating disc electrode surface. After the solvent removal by evaporation at 90 °C, BTMA-MD particles were uniformly distributed on the GCE support in the form of a thin layer. The obtained electrodes with hybrid organic–inorganic interfaces were used as working electrodes.

2.3. Methods

2.3.1. Characterization of samples

The characterization of synthesized BTMA-MDs included chemical and phase analysis and investigation of textural properties. The BTMA-MD samples were checked for their carbon, hydrogen, and nitrogen contents using a Vario EL III device (Hanau Instruments GmbH, Germany). X-ray diffraction (XRD) patterns of the powders of Na-MD and the series of BTMA-MD were obtained using a Philips PW 1710 X-ray powder diffractometer (Philips, Eindhoven and Almelo, The Netherlands) with a Cu anode (λ=0.154178 nm). The type of smectite was determined by submitting raw clay to the Greene-Kelley test [29, 30]. The test consisted of recording XRD difractogramms of appropriately prepared oriented samples. The raw clay was treated with LiCl in order to obtain Li-saturated sample. The procedure included rinsing with deionized water until no trace of chloride was detected by silver nitrate test. The oriented sample was places on a pure silica glass slide, heated overnight at 300 °C and subsequently saturated with ethylene glycol.

FTIR spectra of the Na-MD and different BTMA-MDs were registered using a Thermo Nicolet 6700 FT-IR Spectrophotometer. The KBr pressed disc technique (2 mg of sample and 200 mg of KBr) was used.

Nitrogen adsorption-desorption isotherms were obtained at -196°C using a Sorptomatic 1990, Thermo Finnigan. The samples were outgassed at 80 °C during 10 h. Textural parameter values were calculated according common methods [31]. Specific surface area, S_{BET} was calculated according to the three parameter Brunauer, Emmett, Teller method. Total pore volume, $V_{0.98}$, was calculated according to the Gurvitsch method. Mesopore volume V_{mes}^{BJH}, was obtained according to the Barrett, Joyner, Halenda method. To distinguish between micropores and external surface area the t-plot method was applied [31]. As a standard reference t-curve the Harkins and Jura relation was used.

2.3.2. Adsorption of BTMA on Na-enriched clay

Prior to organomodification the adsorption of BTMA cations on Na-MD was tested. The amount of introduced BTMA cations varied in the interval equivalent to 0.0-2.0 multiples of CEC value. The procedure was as follows. BTMA bromide solutions (40.00 cm^3) of appropriate concentrations were added to 10.00 cm^3 of 1 % (w/w) Na-MD suspension. The prepared BTMA/clay suspensions were shaken for 24 h at 25 °C in a thermostated shaker (Memmert WNE 14 and SV 1422). Supernatants were separated by centrifugation at 17000 rpm for 30 min (Centrifuge Heittech Eva 21). The concentrations of BTMA were determined by measuring the absorption at λ_{max}=262 nm using a UV–Vis spectrophotometer (Thermo Electron Nicolet Evolution 500 UV–Vis).

2.3.3. Adsorption of p-NP on BTMA clays

In order to find correlation between electrochemical behavior of electrodes based on here investigated clay from locality Mečji Do and our previous findings using BTMA modified clay from Bogovina [32] the adsorption of p-NP on BTMA-clays from these localities was performed. The adsorption of 0.2 mM in 0.1 M H$_2$SO$_4$ onto 100 mg 1.0 BTMA-MD and 1.0 BTMA-B (the latter being organoclay obtained in the same manner as 1.0 BTMA-MD but using Bogovina clay) was performed during 24 h in a thermostated shaker at 25 °C. The spectra of p-NP were obtained using Thermo Electron Nicolet Evolution 500 UV-Vis. Since UV-Vis spectra of p-NP vary with pH, prior to every UV-Vis measurement, pH of the supernatant solution was adjusted to pH=3. The calibration curve for p-NP was obtained at λ_{max}=317 nm with the coefficient

6

of determination (R^2) > 0.9999. The acidity of pH=3 was chosen to keep *p*-NP in the molecular state.

The amount of adsorbed *p*-NP at time *t* - q_t (mmol g^{-1}), was calculated from the following mass balance relationship:

$$q_t = (C_t - C_0) \, v \, / \, m_{adsorb} \tag{1}$$

where: v is the volume of solution, while C_0 and C_t (mol dm^{-3}) are the initial and the solution concentrations after adsorption time *t*, respectively.

2.3.4. Electrochemical investigations

For the electrochemical investigations a three-electrode all glass cell was employed. Prepared Na-MD and BTMA-MD modified GCEs were used as the working electrode. The reference electrode was Ag/AgCl in 3 M KCl while platinum foil was the counter electrode. The device used for the electrochemical measurements was a 797 VA Computrace, Metrohm (Herisau Switzerland). Cyclic voltammograms (CV) were recorded at the potential scan rate of 10 mVs^{-1}. The BTMA-MD based electrodes were investigated in 0.1 M H_2SO_4 solution. The Differential Pulse Voltammetry (DPV) measurements were performed at the following conditions: scan rate: 10 mVs^{-1}; pulse amplitude: 50 mV and pulse time: 0.05 s.

3. RESULTS AND DISCUSSION

3.1. Adsorption of BTMA on Na-enriched clay

The results of the equilibrium adsorption of BTMA on Na-MD are presented as the relationship between introduced and adsorbed amount of BTMA cations (Fig. 1).
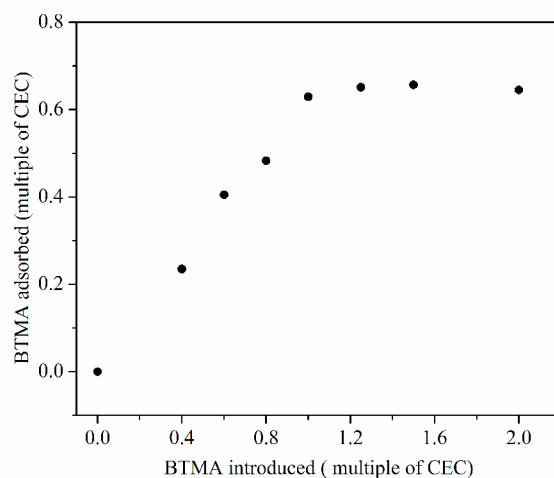
7

Fig. 1. The relationship between introduced and adsorbed amount of BTMA cations.

The BTMA adsorption isotherm was linear for the added amounts that correspond to values between 0.2 and 1.0 times of CEC, but did not reach full saturation of the exchange sites even from the solutions containing an excess of BTMA. The amount of adsorbed BTMA was approximately the same for all added amounts of BTMA that correspond to the values between 1.0 and 2.0 times of CEC.

3.2. Sample characterization

The contents of C, H and N in the obtained BTMA-MDs were analyzed and the results are shown in Table 2. The theoretical values of the elements were calculated according to the CEC value and applied BTMA loading.

Table 2. The elemental analysis of BTMA-MDs.

Sample	Calculated values			Experimental values		
	C	H	N	C	H	N
				mass %		
0.2 BTMA-MD	1.8	0.2	0.2	2.0	0.2	0.2
0.5 BTMA-MD	4.5	0.6	0.5	4.8	0.5	0.6
1.0 BTMA-MD	8.5	1.2	1.0	6.7	0.6	0.8
2.0 BTMA-MD	15.4	2.1	1.8	6.6	0.6	0.8

8

The results indicate that the difference between the calculated and experimental values was very small in the case of organoclays where the introduced BTMA amounts were 0.2 and 0.5 multiples of the CEC value. On the other hand, for the samples modified with BTMA amounts corresponding to 1.0 and 2.0 times of the CEC value, the contents of C, H and N were approximately the same. In both of the cases approx. 76 % of exchangeable cations in Na-MD were replaced by BTMA cations. Full saturation of the exchange sites was not reached even from the solutions containing an excess of BTMA cations. This result is in accordance with the results obtained from the adsorption isotherm (Fig. 1). Other authors have reported similar findings [33, 34].

Since it was proven that 1.0 BTMA-MD and 2.0 BTMA-MD do not differ in the amount of incorporated BTMA cations 2.0 BTMA-MD was not considered in further investigations.

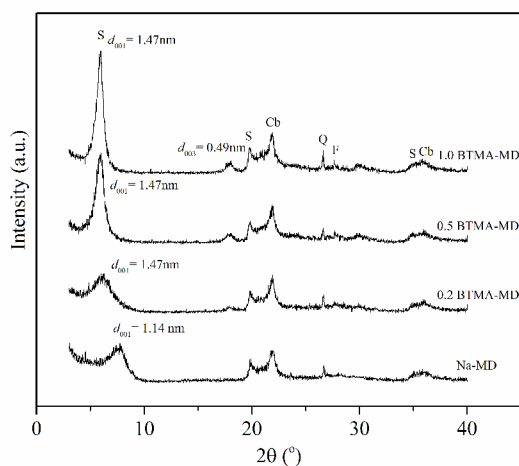The XRD patterns of Na-MD and the series of different BTMA-MD samples are given in (Fig. 2.)

Fig. 2. XRD of investigated clays (S = Smectite, Cb = Cristobalite, F = Feldspar, Q = Quartz).

Na-MD dominantly consisted of smectite with minor quantities of associated minerals like cristobalite, feldspar and quartz [35, 36]. The d_{001}-values of all of the organoclay materials were larger than that of the Na- enriched bentonite. This indicated that the interlamellar spacing of smectite was expanded by the intercalated BTMA cations. The d_{001} value of 1.47 nm, obtained for all BTMA-MD samples, corresponds to monolayer arrangement of BTMA cations between smectite layers. Monolayer arrangement is in

9

this case expected since it is characteristic for short-chain alkylammonium ions [11]. In the diffractograms of BTMA-MDs the peak corresponding to 003 reflection of smectite was also identified. The intensity of this peak increased with BTMA loading.

The presence of clay minerals from smectite group was unambiguously confirmed by XRD. In order to determine the prevailing mineral of the smectite group, the Green–Kelly test [29, 30] was performed. Beidellite and montmorillonite are dioctahedral 2:1 minerals of the smectite minerals group. The distinction between these two minerals is made according to the origin of structural charge. The structural charge of beidellite is due to the substitution of Al^{3+} for Si^{4+} in smectite tetrahedral sheets, while that of montmorillonite is due to Mg^{2+} for Al^{3+} substitution in smectite octahedral sheets. The Green–Kelly test [29, 30] is based on this structural difference. Namely, Li^+ ions from interlamellar region tend to migrate into octahedral vacancies and occupy vacant octahedral sites, thereby neutralizing octahedral sheet charge. Therefore, smectite with octahedral charge (montmorillonite) becomes non-expandable after the Green-Kelly test, whereas smectite with tetrahedral charge (beidellite) does not lose its expandability upon the Li^+-treatment. The result of the Greene–Kelley test performed on raw clay from Mečji Do is given in Fig. 3.
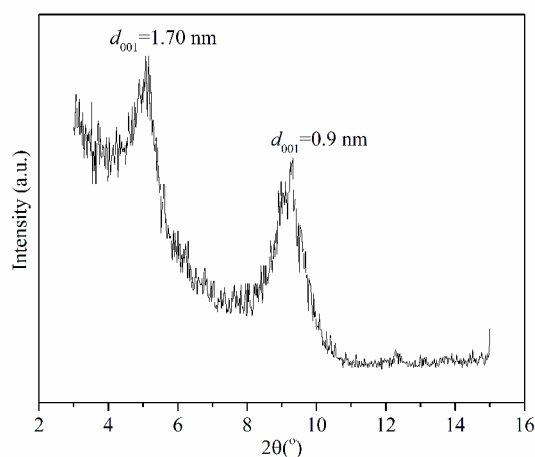

Fig. 3. XRD of raw clay form Mečji Do, treated with LiCl, oriented, heated at 300 °C and saturated with ethylene glycol (Greene–Kelley test).

Two 001 reflections at 1.70 nm and 0.96 nm were observed in the diffractogram presented in Fig. 3, confirming the presence of beidellite and montmorillonite, respectively. The relative amounts of these clay minerals were estimated from their

10

corresponding peak areas. The results showed that the montmorillonite:beidellite ratio was approx. 60:40.

The FTIR spectra of all samples were recorded from 4000 to 400 cm⁻¹. In order to emphasize differences due to modification, only the spectra of the representative materials (Na-MD and 1.0 BTMA-MD) are presented in Fig. 4a. The parts of particular interest of all spectra are enlarged in Figs. 4b-4d.
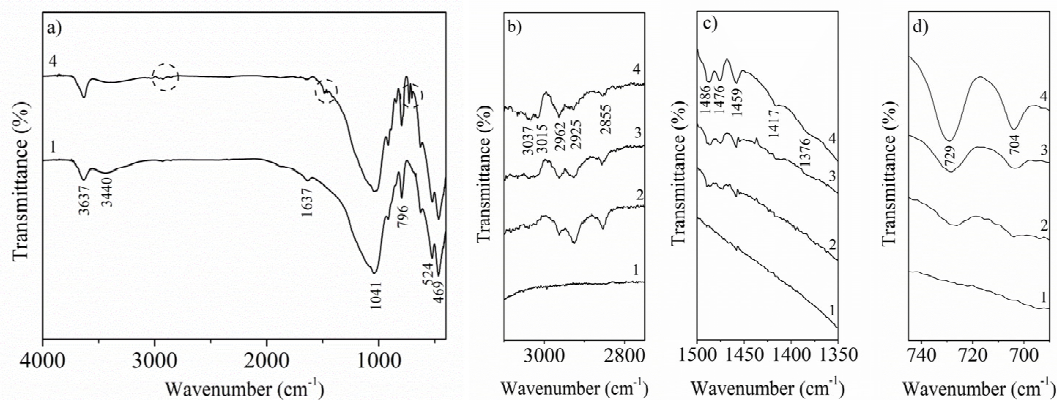

Fig. 4. FTIR spectra of (1) Na-MD, (2) 0.2 BTMA-MD, (3) 0.5 BTMA-MD and (4) 1.0 BTMA-MD: a) 4000-400 cm⁻¹, b) 3100-2750 cm⁻¹, c) 1500-1400 cm⁻¹ and d) 750-690 cm⁻¹.

General shape of all spectra was similar. The bands observed in the Na-MD spectrum were present in the spectra of the BTMA-MDs as well. These bands can be assigned to smectite, crystobalite and water. Additional bands appeared in the spectra of all BTMA-MDs. The following bands can be ascribed to smectite. The broad band at about 3637cm⁻¹ can be assigned to stretching vibrations of hydroxyl group in different environments (AlAlOH, AlMgOH, AlFeOH). The bands at 916, 883 and 844 cm⁻¹ can be assigned to the corresponding bending vibrations. The band at ≈ 1040 cm⁻¹ can be assigned to ν(Si-O-Si). The crystobalite Si-O-Si originating vibrations occurred at 796 and 626 cm⁻¹. The broad vibration bands around 3440 and 1640 cm⁻¹ can be attributed to stretching and banding H-O-H vibrations of interlayer water [37-39].

Beside previously assigned bands, additional absorption bands characteristic for BTMA cations appeared in the FTIR spectra of BTMA-MDs. The incorporation of BTMA is clearly supported by the FTIR-spectra in the 3100-2750 cm⁻¹ (Fig. 4b), 1500-1350 cm⁻¹ (Fig. 4c) and 750-690 cm⁻¹ (Fig. 4d) regions. In these spectroscopic regions the C-H

11

originating vibrations characteristic for organic compounds were detected. In these regions the OH, Si–O, Al–O and Mg–O vibrations of the clay framework, as well as those of the adsorbed water, did not appear and, therefore, did not overlap with the C-H bands of the exchanged organic cations. The intensity of these bands increased with the increase of BTMA loading. In the 3100-2750 cm^{-1} region, where C-H vibrations are expected to appear, very weak bands at 2925 and 2962 cm^{-1} that correspond to aliphatic C-H$_{as}$ stretching vibrations occurred. The band at 2855 cm^{-1} can also be assigned to aliphatic C-H$_{as}$ stretching vibration, while aromatic C-H stretching vibrations were registered at 3015 and 3037 cm^{-1} [40]. In the spectra of BTMA-MDs (Fig. 4c) the bands originated from phenyl ring vibrations were the bands at 1486 and 1476 cm^{-1} that can be assigned to ν_{as}C–C(Ar). The 1459 and 1417 cm^{-1} bands can be assigned to δ_{as}CH$_2$ and δ_sCH$_2$, respectively. The band assigned to the bending vibrations of -CH$_3$ in the ammonium head group appeared at 1376 cm^{-1} [23]. The bands in the 750-690 cm^{-1} region (Fig. 4b) in the BTMA-MDs spectra can be assigned to δ_{opp} C-H(Ar) and indicated the presence of 5 H atoms in benzene ring. This implied that monosubstituted benzene derivate was present in BTMA-MDs [41]

Nitrogen adsorption-desorption isotherms of Na-MD and BTMA-MDs are presented in Fig. 5, while textural properties calculated from these isotherms are presented in Table 3.
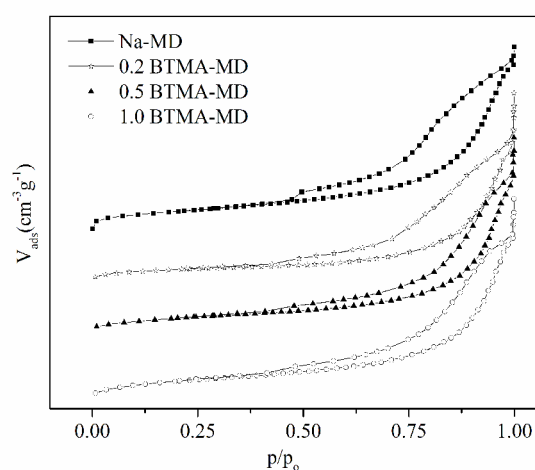

Fig. 5. The N$_2$ low temperature adsorption-desorption isotherms of investigated samples.

The N$_2$ low temperature adsorption-desorption isotherms of all investigated samples belong to the Type II isotherms according to the IUPAC classification [31].

12

Table 3. Selected textural properties.

Sample	S_{BET} [m^2g^{-1}]	$V_{0.98}$ [cm^3g^{-1}]	V_{mes}^{BJH} [$cm^3 g^{-1}$]	S_{ext} [m^2g^{-1}]	V_{mic} [$cm^3 g^{-1}$]	S_{mic} [m^2g^{-1}]
Na-MD	101	0.265	0.272	82	0.008	19
0.2 BTMA-MD	67	0.210	0.232	50	0.004	17
0.5 BTMA-MD	68	0.227	0.236	58	0.003	10
1.0 BTMA-MD	86	0.248	0.250	72	0.005	14

Where: S_{BET} – specific surface area (3-parameter BET equation); $V_{0.98}$ – total pore volume; V_{mes}^{BJH} - mesopore volume (Barrett, Joyner, Halenda method), S_{ext}- external surface area (t-plot method), V_{mic} micropore volume (t-plot method) and S_{mic} – specific micropore volume ($S_{BET} – S_{ext}$)[31].

All values calculated for the textural properties of the BTMA-MDs were smaller than the corresponding values for Na-MD. With the increase of BTMA loading these values approached the values obtained for Na-MD.

The presence of micropores affected the S_{BET} values. The t-plot method enabled the determination of the influence of microporosity on these values. All samples can be regarded as predominantly mesoporous.

Smectites have the capability of uptaking larger organic cations into interlamellar region. Depending on the alkyl chain length, CEC and organic cation loading different arrangements – from pillar-like structures to complete filling of interlamellar region – can be obtained. Both of the structures keep smectite layers apart and affect textural properties including S_{BET} [42, 43]. The overlapping of influences of both of the structures can be deduced from the results presented in Table 3.

3.3. *Electrochemical investigations*

The electrochemical behavior of *p*-NP on the Na-MD and BTMA-MD based electrodes was studied using multisweep cyclic voltammetry. According to the previous investigation of *p*-NP electro-oxidation on BTMA-clay based electrodes synthesized using bentonite clay from Bogovina deposit, a well pronounced signal was obtained in 0.1 M H_2SO_4 as a supporting electrolyte [32]. Therefore, the electrochemical response of the MD clay based electrodes in the oxidation of *p*-NP was here investigated at the same experimentalin 0.1 M H_2SO_4 as a supporting electrolyte conditions.

First, the electrochemical behavior of Na–MD and the series of BTMA-MD modified electrodes in acidic media was investigated. Among the investigated electrodes, the steady state cyclic voltammograms of the Na-MD and 1.0 BTMA-MD were chosen to be shown in Fig. 6 as the representative ones, since these are the materials with the zero and the highest BTMA loading. The electrochemical reaction was studied in wide potential range, from hydrogen evolution at $\approx$ –0.3 V to oxygen evolution at $\approx$ 1.5 V. Multifold cycling was required in order for steady state cyclic voltammograms (CV) to be obtained.
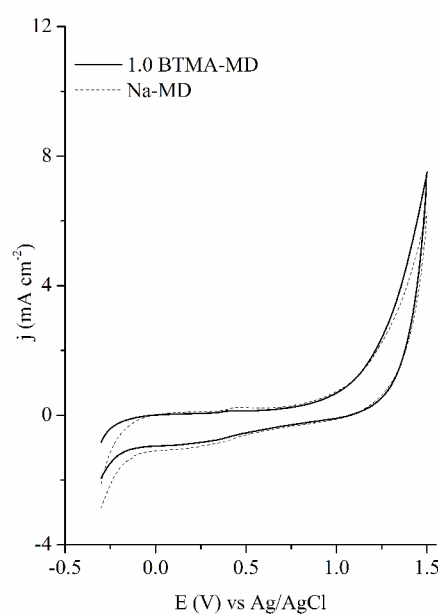

Fig. 6. Steady state CVs of the Na-MD and 1.0 BTMA-MD based composite electrodes in 0.1 M H_2SO_4. The scan rate was 10 mVs^{-1}.

Vertical shift between the curves corresponding to opposite polarization directions was very well pronounced. Such behavior is characteristic for electrodes with high surface area that gives rise to interfacial capacitance [44]. The CVs recorded for the Na-MD and 1.0 BTMA-MD electrodes showed only a capacitive current.

Freshly prepared electrodes were cycled in 10 mM p-NP in 0.1 M H_2SO_4 as supporting electrolyte. Ten successive cycles obtained in p-NP containing solutions for each examined electrode are presented in Fig. 7. The CV of the bare GCE in p-NP containing solution is also presented in Fig. 7a.
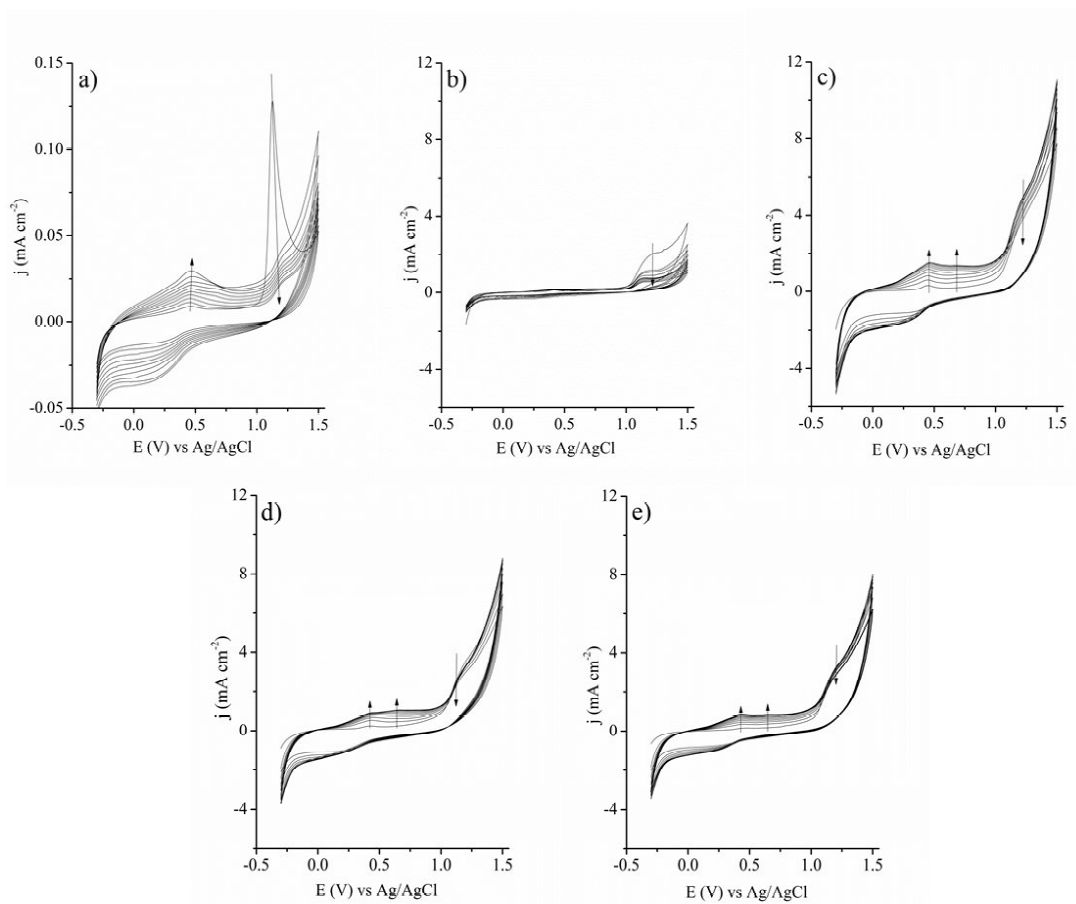
14

Fig. 7. CVs in 10 mM *p*-NP+0.1 M H$_2$SO$_4$ of (a) bare GCE electrode (80 times enlarged scale) and composite clay-based electrodes: (b) Na-MD; (c) 0.2 BTMA-MD; (d) 0.5 BTMA-MD; and (e) 1.0 BTMA-MD. The scan rate was 10 mV s^{-1}. Arrows indicate changes during cycling.

During the anodic sweep from −0.3 to +1.5 V, the *p*-NP oxidation wave was registered on all investigated electrodes at ≈ 1.2 V (Fig. 7.). The oxidation peak appeared at somewhat higher potential value than those typically reported for the oxidation of *p*-NP (1.1 V vs. Ag/AgCl) [45, 46]. The obtained current densities at *p*-NP oxidation wave in the first and tenth cycle are summarized in Table 4.

Table 4. Current densities at *p*-NP oxidation wave in the first (I) and tenth (X) cycle and relative decrease of current density after ten cycles for all investigated electrodes.

Sample	j_I[mA cm^{-2}]	j_X[mA cm^{-2}]	$(j_I\text{-}j_X)/j_I$ [%]
Bare GCE	0.13	0.02	84.6
Na-MD	2.03	0.56	72.4
0.2 BTMA-MD	4.84	3.70	23.6
0.5 BTMA-MD	3.65	3.06	16.7
1.0 BTMA-MD	3.36	3.00	10.8

As expected in the case of the bare GCE the shape and height of the oxidation peak dramatically changed after the first scan. The currents obtained for the bare GCE were 15-37 times lower than the currents obtained for the composite clay GCEs. The bare GCE displayed a rapid loss of activity due to the formation of a polymeric passivation layer [47].

Based on the results presented in Table 4, it can be stated that the current densities related tos *p*-NP oxidation for the Na-MD and BTMA-MD-based electrodes were of the same order of magnitude. The incorporation of BTMA into smectite led to the increase of the current density. After ten completed cycles the activity of the composite electrodes decreased the most for the Na-MD based electrode. The BTMA-MD electrodes showed good stability during ten successive cycles. The current density for the *p*-NP oxidation wave at ≈ 1.2 V slightly decreased with the increase of BTMA loading, while the electrode stability increased in the opposite manner.

During the *p*-NP oxidation a series of products was obtained, and registered as the appearance of broad waves at ≈ 0.5 V. According to earlier reports [48-50], it seems reasonable to assume that *p*-NP oxidation reactions are initiated by the oxidation that yields 4-nitrophenoxy radical and the subsequent oxidation of this radical to the corresponding nitrophenoxy cation (Fig. 8).
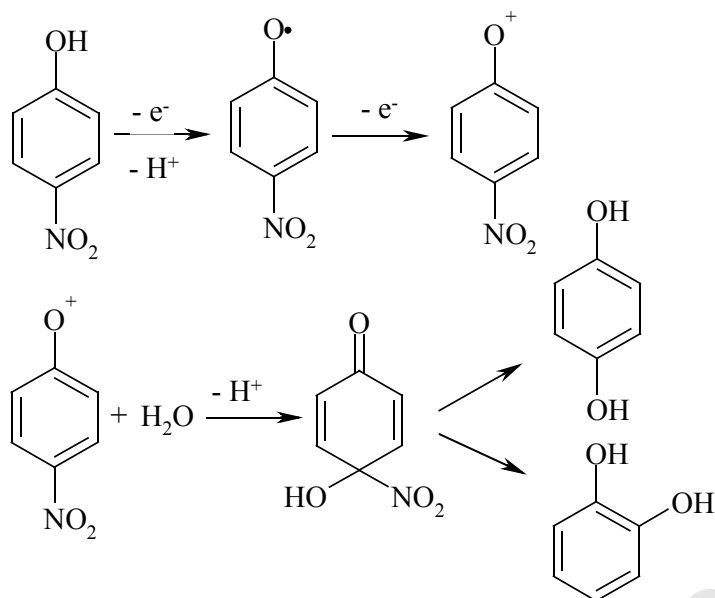
16

Fig. 8. Possible *p*-NP oxidation pathways.

Both nitrophenoxy radical and nitrophenoxy cation are very reactive and can couple to form polymers or undergo other chemical transformations. Chemical transformations include the release of nitro group (or substitution with hydroxyl groups) leading to the formation of non-nitrogenated phenolic or quinonic intermediates. Oturan et al. [51] unequivocally identified by HPLC and GC-MS methods that major intermediary degradation products of *p*-NP are hydroquinone, benzoquinone, 4-nitrocatechol, 1,2,4-trihydroxybenzene and 3,4,5-trihydroxy- nitrobenzene. Safavi *et al.* [2] electrochemically confirmed the occurrence of hydroquinone and catechol in phenol electrooxidation process. Therefore, the peaks registered at 0.43 V and 0.63 V (indicated in Fig. 7 c-7e) were assigned to the oxidation of these species to *p*-benzoquinone and *o*-benzoquinone, respectively. For the BTMA-MD containing electrodes Fig. 7 revealed the increase of the current density of these peaks during cycling. On the other hand, in the CV of the Na-MD based electrode these peaks were negligible. This finding together with rapid electrode fouling suggested that the most dominant pathway of p-NP oxidation on the Na-MD based electrode was the formation of polymeric products.

The same shape of the cyclic voltammograms (Fig. 7) of all investigated BTMA-MD electrodes indicated the existence of identical oxidation-reduction processes. The results

in Fig. 7 provide the information on the nature of the process that occurred on the investigated electrodes. Two trends were observed that lead to complementary conclusions. The first trend is related to the stability of electrodes, expressed as smaller decrease of current density of *p*-NP oxidation during cycling that had the following order: 0.2 BTMA-MD < 0.5 BTMA-MD < 1.0 BTMA-MD. The increase of current density of the oxidation waves corresponding to hydrohinone and catehol oxidation that followed the opposite order is the second trend. Both trends confirmed that with the increase of BTMA loading the polymerization pathway had less significance.

There is a difference between the electrochemical behavior of the composite electrodes based on BTMA-modified clay from Mečji Do and previously reported behavior of the electrodes of the same type based on clay from Bogovina deposit [32]. The latter were sensitive in the process of the electrooxidation of *p*-NP, but were easily deactivated. Their complete deactivation occurred after five successive cycles.

In order to provide explanation for observed differences the in electrochemical behavior additional experiment was performed. The ability of clays to adsorb and preconcentrate analyte is significant for their application as composite electrodes in electrooxidation process. Therefore the adsorption of *p*-NP on Mečji Do and Bogovina BTMA-modified clay was performed. Since the best stability can be ascribed tto the composite electrode based on 1.0 BTMA-MD, this material and its analogue from Bogovina (1.0 BTMA-B) were tested as *p*-NP adsorbents (Fig. 9).
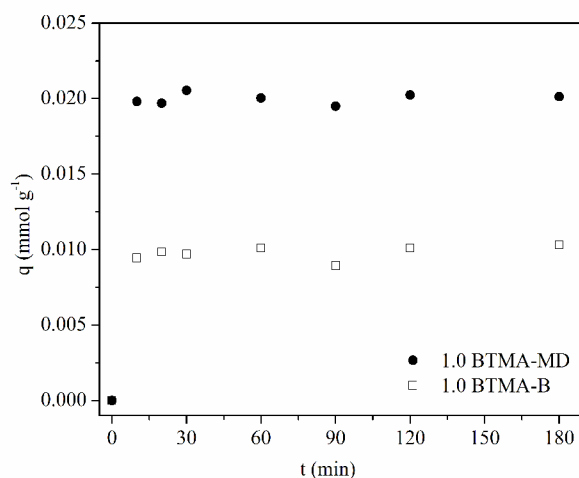

Fig. 9. The effect of contact time on the adsorption of *p*-NP onto clays from different localities modified with BTMA.

As expected the adsorptive properties of two investigated organoclays differed. 1.0 BTMA-MD adsorbed twice the amount of *p*-NP that was adsorbed on 1.0 BTMA-B. In order to explain the differences in the adsorptive and electrochemical behavior of BTMA-modified clays from Mečji Do and Bogovina localities, the difference in the structure of smectite (their main clay mineral) will be discussed.

According to the Greene-Kelly test (Fig. 3), it was determined that mortmorillonite:beidelite ratio in bentonite clay from Mečiji Do locality is approx. 60:40, while bentonite clay from Bogovina locality contains smectite with mortmorillonite:beidelite ratio of approx. 10:90 [30]. Although, montmorillonite and beidellite have very similar structures and properties, it seems that the position of structural charge in them plays important role. Yamada et al. [52] suggested a model of distribution of negative layer charge which greatly depends on the montmorillonite/bedellite ratio. Structural charge influences the adsorption and distribution of alkylammonium cations [53]. It is possible that the difference in the position of structural charge (beidellite/montmorillonite) influences the adsorptive and therefore electrochemical behavior of the investigated materials.

In order to further characterize 1.0 BTMA-MD, which showed to be the most promising electrode material among the investigated ones, additional electrochemical measurement was conducted. The technique of Differential Pulse Voltammetry (DPV) yields well defined peaks at very low concentration levels, which renders it a very sensitive electroanalytical technique. The investigation of the 1.0 BTMA-MD electrode sensitivity towards *p*-NP was performed by DPV. Aliquots of *p*-NP were successively added to a 0.1 M H_2SO_4 solution and DPV voltammograms were recorded. The calibration curve obtained from the DPV data is shown in Fig. 10.
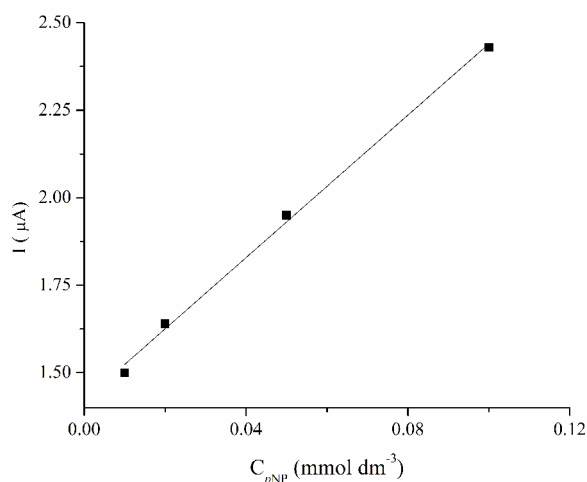
19

Fig. 10. Calibration curve for *p*-NP on composite 1.0 BTMA-MD based electrode.

Anodic peak currents were linearly correlated to the concentration of *p*-NP over the concentration range from 0.01 mmol dm^{-3} to 0.1 mmol dm^{-3}. The detection limit was determined from the 3S$_a$/b ratio, where S$_a$ is the estimate of standard deviation in the intercept with *y* axis of at least three calibration curves and b is the slope of the analytical curve [54]. The detection limit determined for the 1.0 BTMA-MD electrode was 0.007 mmol dm^{-3}. Results comparable with those in the present study have been reported by other researchers [55, 56].

4. CONCLUSION

A series of benzyltrimethylammonium clays (BTMA–MD) with different BTMA loading was prepared using bentonite clay from seldom investigated locality Mečji Do in Serbia. Per g of clay BTMA was introduced in the amounts equal to 0.2, 0.5, 1.0 and 2.0 times multiplied cation exchange capacity (CEC) value. Respective materials were denoted as 0.2–1.0 BTMA-MD. For 0.2 BTMA-MD and 0.5 BTMA-MD the incorporation of introduced BTMA in the interlamellar region was quantitative. In the case of the samples modified with the amounts of BTMA cations corresponding to 1.0 and 2.0 times of CEC value approx. 76 % of exchangeable cations were replaced with BTMA cations. The XRD data confirmed monolayer arrangement of BTMA intercalated in smectite for all BTMA loadings. Beside vibrational bands originated from the clay, absorption bands assigned to organic C-H related vibrations,

characteristic for organic compounds, were detected in the FTIR spectra of BTMA-MDs. The intensity of these bands increased with the increase of BTMA loading. All calculated values for textural properties of BTMA-MDs were smaller than the corresponding values for Na-MD. With the increase of BTMA loading these values approached those obtained for Na-MD. Composite glassy carbon electrodes (GCEs) containing each of the modified clays separately, were tested in the electrooxidation of *p*-NP in acidic media. Oxidation of *p*-NP occurred at ≈1.2 V vs. Ag/AgCl for all the investigated electrodes. The results indicated that the incorporation of BTMA into smectite enhanced the electrode stability toward the electrooxidation of *p*-NP in comparison with the bare GCE and the composite GCE containing Na-enriched clay. The current density for the *p*-NP oxidation wave slightly decreased with the increase of BTMA loading. On the other hand the electrode stability was significantly improved with the increase of BTMA loading.

Acknowledgments

REFERENCES

[]] Toxic Substance Control Act, US Environmental Protection Agency,Washington, DC, 1979.

[2] A. Safavi, N. Maleki, F. Tajabadi, Highly stable electrochemical oxidation of phenolic compounds at carbon ionic liquid electrode, Analyst 132 (2007) 54-58.

[3] A. Niazi, A. Yazdanipour, Spectrophotometric simultaneous determination of nitrophenol isomers by orthogonal signal correction and partial least squares. J. Hazard. Mater. 146 (2007) 421-427.

[4] M. Guidotti, G. Ravaioli, M. Vitali, Total p-nitrophenol determination in urine samples of subjects exposed to parathion and methyl parathion by SPME and GC/MS. HRC-J. High Resolut. Chromatogr. 22 (1999) 628–630.

[5] R. Belloli, B. Barletta, E. Bolzacchini, S. Meinardi, M. Orlandi, B. Rindone, Determination of toxic nitrophenols in the atmosphere by high-performance liquid chromatography, J. Chromatogr. A, 846 (1999) 277–281.

[6] R.W. Murray, Introduction to the chemistry of molecularly designed electrode surfaces, in: R.W. Muray (Ed.), Molecular Design of Electrode Surfaces, Techniques of Chemistry, vol. 22. Wiley and Sons, New York, 1992, pp. 1– 48.

[7] C. Mousty, Sensors and biosensors based on clay-modified electrodes-new trends, Appl. Clay Sci. 27 (2004) 159– 177

[8] I. N. Rodríguez, J. A. Muñoz Leyva, J. L. Hidalgo, H. de Cisneros, Use of a carbon paste modified electrode for the determination of 2-nitrophenol in a flow system by differential pulse voltammetry, Anal. Chim. Acta. 344 (1997) 167-173

[9] H. L. Tcheumi, I. K. Tonle, E. Ngameni, A. Walcarius, Electrochemical analysis of methylparathion pesticide by a Gemini surfactant-intercalated clay-modified electrode, Talanta 81 (2010) 972–979.

[10] J. K. Wagheu, C. Forano, P. Besse-Hoggan, I. T. Kenfack, E. Ngameni, C. Mousty, Electrochemical determination of mesotrione at organoclaymodified glassy carbon electrodes, Talanta 103 (2013) 337–343.

[11] F. Bergaya, G. Lagaly, General Introduction: Clays, Clay Minerals, and Clay Science, in: F. Bergaya, G. Lagaly (Eds.), Developments in Clay Science – Volume 5A, Handbook of Clay Science, second ed., Elsevier Ltd, Amsterdam, 2013, pp. 1-19.

[12] J. C. K. Mbouguen, I. T. Kenfack, A. Walcariusc, E. Ngamenia, Electrochemical response of ascorbic and uric acids at organoclay film modified glassy carbon electrodes and sensing applications, Talanta 85 (2011) 754–762.

[13] S. Arellano-Cárdenas, S. López-Cortez, M. Cornejo-Mazón, J. C. Mares-Gutiérrez, Study of malachite green adsorption by organically modified clay using a batch method, Appl. Surf. Sci. 280 (2013) 74–78.

[14] A.S. Özcan, B. Erdem, A. Özcan, Adsorption of Acid Blue 193 from aqueous solutions onto BTMA-bentonite, Colloid. Surface A, 266 (2005) 73-81.

[15] M. Majdan, S. Pikus, A. Gajowiak, A. Gładysz-Płaskaa, H. Krzyżanowska, J. Żuk, M. Bujacka, Characterization of uranium(VI) sorption by organobentonite, Appl. Surf. Sci. 256 (2010) 5416–5421).

[16] L. Zhu , X. Ren, S. Yu, Use of cetyltrimethylammonium bromide-bentonite to remove organic contaminants of varying polar character from water, Environ. Sci. Technol. 32 (1998) 3374-3378.

[17] M.N. Carvalho, M. da Motta, M. Benachour, D.C.S. Sales, C.A.M. Abreu, Evaluation of BTEX and phenol removal from aqueous solution by multi-solute adsorption onto smectite organoclay, J. Hazard. Mater. 239–240 (2012) 95–101.

22

[18] J. A. Smith, A. Galan, Sorption of nonionic organic contaminants to single and dual organic cation bentonites from water, Environ. Sci. Technol. 29 (1995) 685-692.

[19] J. A. Smith, P. R. Jaff, C. T. Chlou, Effect of ten quaternary ammonium cations on tetrachloromethane sorption to clay from water, Environ, Sci. Technol. 24 (1990) 1167-1172.

[20] C.C. Wang, L.C. Juang, C.K. Lee, T.C. Hsu, J.F. Lee, H.P. Chao, Effect of exchanged surfactant cations on the pore structure and adsorption characteristics of montmorillonite, J. Colloid Interf. Sci. 280 (2004) 27-35.

[21] Y-H. Shen, Removal of phenol from water by adsorption–flocculation using organobentonite, Water Res. 36 (2002), 1107–1114.

[22] S. Al-Asheh, F. Banat, L. Abu-Aitah, Adsorption of phenol using different types of activated bentonites, Sep. Purif.Technol. 33 (2003) 1–10.

[23] M. Majdan, M. Bujacka, E. Sabah, A. G1adysz-P1aska, S. Pikus,D. Sternik, Z. Komosa, A. Padewski, Unexpected difference in phenol sorption on PTMA- and BTMA-bentonite, J. Environ. Manage. 91 (2009) 195–205

[24] A. Abu Rabi-Stanković, Z. Mojović, A. Milutinović-Nikolić, N. Jović-Jovičić, P. Banković, M. Žunić, D. Jovanović, Electrooxidation of p-nitrophenol on organobentonite modified electrodes, Appl. Clay Sci. 77–78 (2013) 61–67.

[25] S. Hu, C. Xu, G. Wang, D. Cui, Voltammetric determination of 4-nitrophenol at a sodium montmorillonite-anthraquinone chemically modified glassy carbon electrode. Talanta 54 (2001) 115-123.

[26] H. Yang, X. Zheng, W. Huang, K. Wu, Modification of montmorillonite with cationic surfactant and application in electrochemical determination of 4-chlorophenol, Colloid. Surface. B 65 (2008) 281-284.

[27] Environmental Protection Agency, 1986. Method 9080 - Cation exchange capacity of soils (ammonium acetate). Available from http://www.epa. gov/osw/hazard/testmethods/sw846/pdfs/9080.pdf (verified 14 March 2013).

[28] N. Jović-Jovičić, A. Milutinović-Nikolić, P. Banković, Z. Mojović, M. Žunić, I. Gržetić, D. Jovanović, Organo-inorganic bentonite for simultaneous adsorption of Acid Orange 10 and lead ions, Appl. Clay Sci. 47 (2010) 452–456.

[29] R. Greene-Kelly, The identification of montmorillonoids in clays, J. Soil Sci. 4 (1953) 233-237.

[30] T. Novaković, Lj. Rožić, S. Petrović, A. Rosić, Synthesis and characterization of

23

acid activated Serbian smectite clays obtained by statistically designed experiments, Chem. Eng. J. 137 (2008) 436-442.

[31] F. Rouquerol, J. Rouquerol, K. Sing, Adsorption by powders and porous solids. Academic Press, London, 1999.

[32] A. Abu Rabi-Stanković, A. Milutinović-Nikolić, N. Jović-Jovičić, P. Banković, M. Žunić, Z. Mojović, D. Jovanović, p-nitrophenol electro-oxidation on a BTMA$^+$-bentonite modified electrode, Clay Clay Miner. 60 (2012) 291–299.

[33] S.-M. Koh, J. B. Dixon, Preparation and application of organo-minerals as sorbents of phenol, benzene and toluene, Appl. Clay Sci. 18 (2001) 111–122.

[34] T. Polubesova, G. Rytwo, S. Nir, C. Serban, L. Margulies, Adsorption of benzyltrimethylammonium and benzyltriethylammonium on montmorillonite: experimental studies and model calculations, Clay Clay Miner. 45 (1997) 834-841.

[35] D.M.C. MacEwan, M.J. Wilson Interlayer and intercalation complexes of clay minerals, in: G.W Brindley, G. Brown (Eds.), Crystal structures of clay minerals and their X-ray identification, Mineralogical Society, London, 1980, pp. 197-248.

[36] International Center for Diffraction Data - Joint Committee on Powder Diffraction Standards, Powder diffraction data, Swarthmore, PA, USA, 1990.

[37] J. Madejová, P. Komadel, B. Čičel, Infrared study of octahedral site populations in smectites, Clay Miner. 29 (1994) 319-326.

[38] J. Madejová, P. Komadel, Baseline studies of the clay minerals society source clays: infrared methods, Clay Clay Miner. 49 (2001) 410–432.

[39] G.E. Christidis, P.W. Scott, A.C. Dunham, Acid activation and bleaching capacity of bentonites from the islands of Milos and Chios, Aegean, Greece, Appl. Clay Sci. 12 (1997) 329–347.

[40] Y. Z. El-Nahhal, J. M. Safi, Adsorption of phenanthrene on organoclays from distilled and saline water, J. Colloid. Interf. Sci. 269 (2004) 265–273.

[41] E. Pretsch, J. Seibl, W. Simon, Tabellen zur strukturafklärung organischer verbindungen mit spektroskopischen methoden, Springer Verlag, Berlin Heidelberg, 1981.

[42] J.-F. Lee, C.-K. Lee, L.-C. Juang, Size effects of exchange cation on the pore structure and surface fractality of montmorillonite, J. Colloid. Interf. Sci. 217 (1999) 172176

24

[43] C.-C. Wang, L.-C. Juang, C.-K. Lee, T.-C. Hsu, J.-F. Lee, H.-P. Chao, Effects of exchanged surfactant cations on the pore structure and adsorption characteristics of montmorillonite, J. Colloid. Interf. Sci. 280 (2004) 27–35.

[44] S. Mentus, Z. Mojović, N. Cvjetičanin, Ž. Tešić, Electrochemical water splitting on zeolite supported platinumclusters, J. New. Mat. Electrochem. Syst. 7 (2004) 213–220.

[45] V. A. de Pedrosa, L. Codognoto, L. A. Avaca, Electroanalytical determination of 4-nitrophenol by square wave voltammetry on diamond electrodes, J. Braz. Chem. Soc. 14 (2003) 530-535.

[46] A. Arvinte, M. Mahosenaho, M. Pinteala, A. M. Sesay, V. Virtanen, Electrochemical oxidation of p-nitrophenol using graphene-modified electrodes, and a comparison to the performance of MWNT-based electrodes, Microchim. Acta 174 (2011) 337–343.

[47] J. Wang, R. Li, Highly stable voltammetric measurements of phenolic compounds at poly(3-methylthiophene)-coated glassy carbon electrodes, Anal. Chem. 61 (1989) 2809–2811.

[48] S. Ammar, N. Oturan, M. A. Oturan, Electrochemical oxidation of 2-nitrophenol in aqueous medium by electro-fenton technology, J. Environ. Eng. Manage. 17 (2007), 89-96.

[49] P. Cañizares, C. Sáez, J. Lobato, M. A. Rodrigo, Electrochemical treatment of 4-nitrophenol-containing aqueous wastes using boron-doped diamond anodes, Ind. Eng. Chem. Res. 43 (2004) 1944-1951.

[50] X. Zhu, S. Shi, J. Wei, F. Lv, H. Zhao, J. Kong, Q. He, J. Ni, Electrochemical oxidation characteristics of p-substituted phenols using a boron-doped diamond electrode, Environ. Sci. Technol., 41 (2007) 6541-6546.

[51] M.A. Oturan, J. Peiroten, P. Chartrin, A.J. Acher Complete destruction of p-nitrophenol in aqueous medium by electro-Fenton method, Environ. Sci. Technol. 34 (2000), 3474-3479.

[52] H. Yamada, H. Nakazawa, K. Yoshioka, T. Fujita, Smectites in the montmorillonite-beidellite series, Clay Miner. 26 (1991) 359-36.

[53] P. Čapková, M. Pospíšil, J. Miehé-Brendlé, M. Trchová, Z. Weiss, R. Le Dred, Montmorillonite and beidellite intercalated with tetramethylammonium cations, J. Mol. Model. 6 (2000) 600 – 607.

[54] J.C. Miller, J.N. Miller, Basic statistical methods for analytical chemistry. Part I. Statistics of repeated measurements, Analyst 113 (1988) 1351–1356.

[55] P. Calvo-Marzal, S.S. Rosatto, P.A. Granjeiro, H. Aoyama, L.T. Kubota, Electroanalytical determination of acid phosphatase activity by monitoring p-nitrophenol, Anal. Chim. Acta 441 (2001) 207-214.

[56] S. Lupu, C. Lete, M. Marin, N. Totir, P.C. Balaure, Electrochemical sensors based on platinum electrodes modified with hybrid inorganic-organic coatings for determination of 4-nitrophenol and dopamine. Electrochim Acta 54(2009):1932-1938.

FIGURE CAPTIONS

Fig. 1. The relationship between introduced and adsorbed amount of BTMA cations.

Fig. 2. XRD of investigated clays diffractograms (S = Smectite, Cb = Cristobalite, F = Feldspar, Q = Quartz).

Fig 3. XRD of raw clay form Mečji Do, treated with LiCl, oriented, heated at 300 °C and saturated with ethylene glycol (Greene – Kelley test).

Fig. 4. FTIR spectra of (1) Na-MD, (2) 0.2 BTMA-MD, (3) 0.5 BTMA-MD and (4) 1.0 BTMA-MD : a) 4000–400 cm^{-1}, b) 3100–2750 cm^{-1}, c) 1500-1400 cm^{-1} and d) 750-690 cm^{-1}.

Fig. 5. The N_2 low temperature adsorption-desorption isotherms of investigated samples.

Fig. 6. Steady state CVs of the Na-MD and 1.0 BTMA-MD based composite electrodes in 0.1 M H_2SO_4. The scan rate was 10 mVs^{-1}.

Fig. 7. CVs in 10 mM p-NP+0.1 M H_2SO_4 of (a) bare GCE electrode (80 times enlarged scale) and composite clay-based electrodes: (b) Na-MD; (c) 0.2 BTMA-MD; (d) 0.5 BTMA-MD; and (e) 1.0 BTMA-MD. The scan rate was 10 mV s^{-1}. Arrows indicate changes during cycling.

Fig. 8. Possible p-NP oxidation pathways.

Fig. 9 The effect of contact time on the adsorption of p-NP onto clays from different localities modified with BTMA.

Fig. 10. Calibration curve for p-NP on composite 1.0 BTMA-MD based electrode.

26

Highlights

➢ Bentonite clay was modified with different benzyltrimethylammonium (BTMA) loadings.

➢ Modified clays were used for synthesis of composite glassy carbon electrode (GCE).

➢ Composite GCEs were tested in the electrooxidation of *p*-nitrophenol (*p*-NP).

➢ The presence of BTMA in composite GCEs enhanced electrode stability.

➢ The electrode stability significantly improved with the increase of BTMA loading.

27